

Spin density distribution in a partially magnetized organic quantum magnet

A. Zheludev,^{1,*} V. O. Garlea,¹ S. Nishihara,^{2,3} Y. Hosokoshi,^{2,3} A. Cousson,⁴ A. Gukasov,⁴ and K. Inoue⁵

¹*Neutron Scattering Sciences Division, Oak Ridge National Laboratory, Oak Ridge, Tennessee 37831-6393, USA.*

²*Department of Physical Science, Osaka Prefecture University, ,Osaka 599-8531, Japan.*

³*Institute for Nanofabrication Research, Osaka Prefecture University, Osaka 599-8531, Japan.*

⁴*Laboratoire Leon Brillouin, CEA-CNRS Saclay, France.*

⁵*Department of Chemistry, Hiroshima University, Hiroshima 739-8526, Japan.*

(Dated: August 7, 2018)

Polarized neutron diffraction experiments on an organic magnetic material reveal a highly skewed distribution of spin density within the magnetic molecular unit. The very large magnitude of the observed effect is due to quantum spin fluctuations. The data are in quantitative agreement with direct diagonalization results for a model spin Hamiltonian, and provide insight on the actual microscopic origin of the relevant exchange interactions.

I. INTRODUCTION

Static spin correlations in low-dimensional and molecular magnets are often severely affected by zero-point quantum spin fluctuations. The simplest and most extreme example is that of an antiferromagnetic (AF) spin dimer, where the spin density distribution $\mathbf{S}(\mathbf{r})$ is strictly zero in the ground state, even in the presence of a small aligning magnetic field. In partially magnetized states of more complex systems one can expect to find exotic non-trivial spin densities that too are strongly modified by quantum fluctuations. Experimental studies of these correlations can be revealing of the underlying physics, and help determine or validate theoretical models used to describe such materials. Below we report a direct measurement of field-induced magnetization densities in the novel organic molecular magnet 2-[2',6'-difluoro-4'-(*N*-*tert*-butyl-*N*-oxyamino)phenyl]-4,4,5,5-tetramethyl-4,5-dihydro-1*H*-imidazol-1-oxyl, F₂PNNNO for short.

This compound is a prototypical spin-tetramer system.^{1,2} Its molecular building block (Fig. 1a) contains only *s*- and *p*- elements, but is nevertheless magnetic, thanks to two unpaired electrons that reside in π^* antibonding molecular orbitals of the nitronyl nitroxide (NN) and the *tert*-butyl nitroxide (tBuNO) groups, respectively. The material crystallizes in an orthorhombic structure, $a = 19.86 \text{ \AA}$, $b = 14.01 \text{ \AA}$ and $c = 13.48 \text{ \AA}$, space group P_{bca} . In the crystal, F₂PNNNO molecules are arranged in pairs, so that their tBuNO groups are close enough for partial orbital overlap, enabling intermolecular magnetic interactions. The result is a two-molecule unit containing four interacting spins (Fig. 1b). A model Heisenberg Hamiltonian for these $S = 1/2$ -tetramers was proposed based on bulk susceptibility and high field magnetization data.² Intra-molecular exchange coupling is ferromagnetic, with $J_F \approx 35 \text{ meV}$. Intermolecular interactions are AF in nature, of magnitude $J_{AF} \approx 5.8 \text{ meV}$.² In agreement with experiment, this model has a unique non-magnetic ground state with total spin $S_{\text{total}} = 0$, and a gap in the excitation spectrum. The magnetization density in the ground state is strictly zero in entire space.

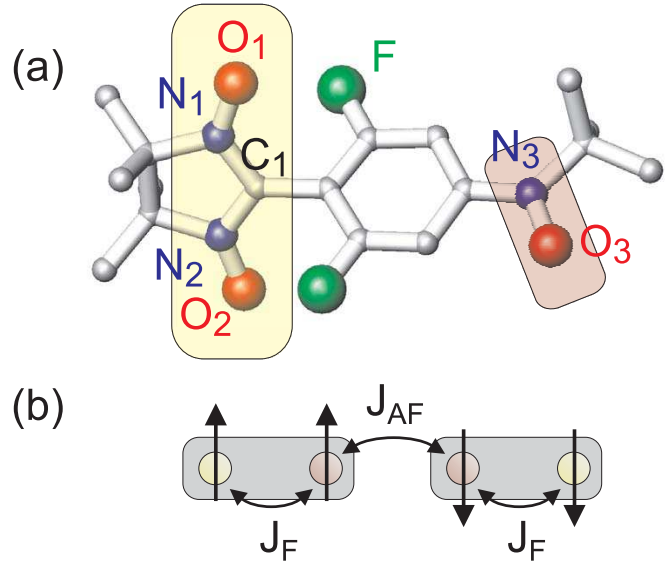


FIG. 1: (Color online) (a) Molecular structure of F₂PNNNO. Hydrogen atoms are not shown. The shaded rectangles represent $S = 1/2$ -carrying unpaired electrons distributed over the nitronyl nitroxide and *tert*-butyl nitroxide groups. (b) A schematic representation of the 4-spin Heisenberg Hamiltonian for a two-molecule F₂PNNNO unit. J_F and J_{AF} are ferro- and antiferromagnetic exchange interactions, respectively. Vertical arrows represent individual spins in the classical ground state $|\uparrow\uparrow\downarrow\downarrow\rangle$. The actual quantum ground state has zero spin density throughout the tetramer.

A non-trivial spin (magnetization) density is only to be found in some of the tetramer's *excited* states. In the presence of an external magnetic field applied along the z axis, the one with the lowest energy has a total spin $S_{\text{total}} = 1$ and a spin projection $S_{z,\text{total}} = +1$. We shall denote this state as $|1, +1\rangle$. By numerically diagonalizing the 4-spin Heisenberg Hamiltonian we find that it actually is a linear combination of four “pure” spin wave functions:

$$|1, +1\rangle = \alpha |\uparrow\uparrow\uparrow\downarrow\rangle + \beta |\uparrow\uparrow\downarrow\uparrow\rangle - \alpha |\downarrow\uparrow\uparrow\uparrow\rangle - \beta |\uparrow\downarrow\uparrow\uparrow\rangle, \quad (1)$$

where $\alpha \approx 0.46$ and $\beta \approx 0.54$. The most striking conse-

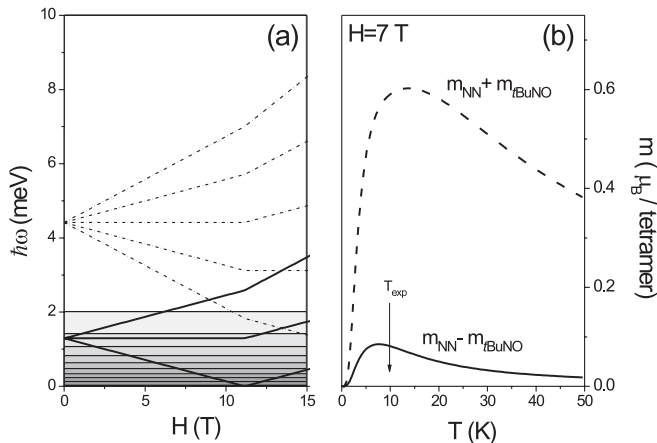


FIG. 2: (a) Calculated field-dependence of the energy levels of an F_2PNNNO spin-tetramer. Heavy solid lines are the lowest energy $S = 0$ and $S = 1$ states. Dashed lines are $S = 2$ states. More excited states are present above 35 meV. The plot is laid over a filled-contour plot of the thermal population function $\exp(-\hbar\omega/T)$ for $T = 10$ K (0.1 contour step). (b) Calculated temperature dependence of the sum (dashed line) and difference (solid line) of the spin populations of the nitronyl nitroxide and *tert*-butyl nitroxide groups. The arrow indicates the experimental temperature.

quence of the quantum-mechanical nature of this state is a skewed spin density distribution $S_z(\mathbf{r})$. The local spin populations of the NN groups are expected to be equal, but different from those of the tBuNO groups. Their ratio R is given by $R = \alpha^2/\beta^2 \approx 1.39$. The central purpose of this work is an experimental detection of this effect.

II. EXPERIMENTAL

To observe this phenomenon, one must first prepare the tetramer in its first excited state. One strategy is to substantially increase the external field. Due to Zeeman effect, the energy of the excited state will decrease, and eventually reach zero at some critical field H_c . At this point it will become the *new* ground state, for which the spin density distribution can be measured. In F_2PNNNO , due to residual inter-tetramer interactions, the transition at H_c is spread out between $H_1 = 9$ T and $H_2 = 15$ T.² While it is certainly possible to perform experiments at $H > H_1$, the equipment available for the present study was limited to fields up to 7 T. For this reason we used a slightly different approach. First, a high field was used to lower the energy of the $|1, +1\rangle$ state as much as possible. The data were then taken at an elevated temperature of $T = 10$ K that made this state partially populated due to thermal fluctuations. Of course, states $|1, 0\rangle$ and $|1, -1\rangle$, as well as other higher-spin states got thermally excited as well. However, at $T = 10$ K thermal populations of higher-spin states are negligible. This is illustrated in Fig. 2(a) that shows the field dependence

of tetramer energy levels calculated using exact numerical diagonalization of the Heisenberg Hamiltonian. The plot is laid over a shaded contour plot of the thermal population function $\exp(-\hbar\omega/T)$. At $H = 7$ T all but the lowest $S = 1$ energy levels are outside the populated region. The $|1, 0\rangle$ state plays no role, as it has $S_z(\mathbf{r}) \equiv 0$. The spin density distribution in $|1, -1\rangle$ is exactly the reverse of that for $|1, +1\rangle$, and does not affect the imbalance between the NN and tBuNO groups. The only adverse effect of the finite- T approach is a reduction of the total magnetization of the tetramer, that ultimately reduces signal strength in any spin density measurement. The actual value of $T = 10$ K was selected to optimize both the total tetramer magnetization and the predicted population difference between the NN and tBuNO groups at $H = 7$ T (Fig. 2b). A full thermodynamic calculation for the 4-spin Hamiltonian predicts $R = 1.32$ for these conditions, just slightly less than the ideal value $R = 1.39$ for a tetramer purely in the $|1, +1\rangle$ state.

Measuring the distribution of about $0.5 \mu_B$ over two molecules with 48 atoms each with angstrom resolution is a formidable experimental challenge. It can only be met by polarized neutron diffraction.³ This technique achieves great sensitivity by exploiting the interference between magnetic and nuclear scattering of neutrons in the crystal. For F_2PNNNO the data were taken at the 5C1 and 6T2 lifting counter diffractometers installed at the Orphe reactor at LLB, using 0.841 \AA and 1.4 \AA neutrons, respectively. Beam polarizations of 91% or 97% were achieved using Heussler-alloy monochromator and supermirror bender. A 20 mg F_2PNNNO single crystal sample was mounted consecutively with the a , b and c axes parallel to the field direction. Sample environment was a split-coil cryomagnet. Overall, 70 independent flipping ratios were measured in magnetic fields $H = 7$ T and $H = 4$ T at $T=10$ K, typically counting 2 hours per reflection on the 5C1 and 30 minutes on the 6T2 diffractometers, respectively. Extracting the corresponding spatial Fourier components of $S_z(\mathbf{r})$ from these data required knowledge of the low-temperature crystal structure. The latter was measured in a single crystal unpolarized neutron diffraction experiment. 3887 independent Bragg intensities were measured for a 5 mg single crystal sample on the 5C2 4-circle diffractometer at Orphe using 0.832 neutrons. Sample environment was a gas flow cryostat, and the data were taken at $T=50$ K. The crystal structure was refined assuming isotropic vibrational parameters for hydrogen atoms, and general anisotropic ones for all other. The resulting least-squares R-factor was 0.089.

III. RESULTS

Inverting the Fourier transform to reconstruct the real-space $S_z(\mathbf{r})$ function is far from straightforward, and prompted us to apply several complimentary approaches. One such tool was the maximum entropy (ME) method.⁴

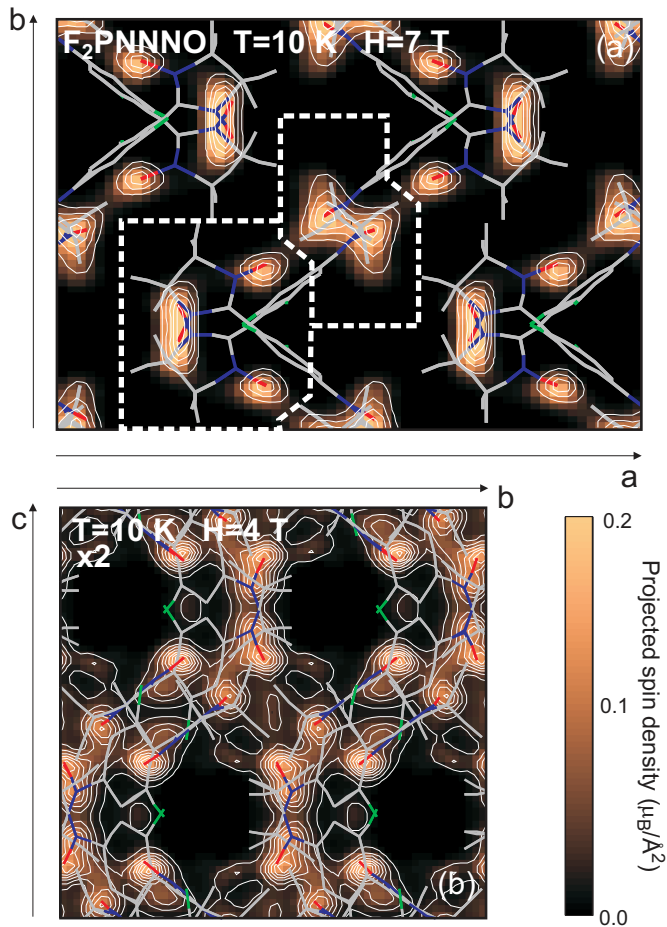


FIG. 3: (Color online) Experimental spin density distribution in a F_2PNNNO spin-tetramer at $T = 10$ K, as reconstructed using the Maximum Entropy method. (a) and (b) are projections onto the (a, b) and (b, c) (crystallographic planes, respectively). Overlaid are skeletal representations of F_2PNNNO molecules as they are positioned within the crystallographic unit cell. Areas outlined with thick dashed lines were used to estimate the spin populations on the nitronyl nitroxide and *tert*-butyl nitroxide groups (see text).

The procedure is model-independent: it uses only the experimental structure factors and crystal symmetry as input, and does not rely on any additional information or assumptions. It is known to be particularly effective at reconstructing 2D projections of $S_z(\mathbf{r})$ onto planes close to the principal scattering plane of the diffractometer.⁵ Results of such reconstructions for F_2PNNNO are shown in Fig. 2. Despite the limited experimental spatial resolution, one immediately sees that the spin density is primarily localized around the N and O atoms. Already at this stage it is possible to get a crude estimate of the redistribution effect. Integrating over the empirically chosen regions outlined in Fig. 2a, we get $R = 1.22$. However, the actual NN/tBuNO spin population imbalance is likely to be more pronounced than suggested by ME. For all its advantages, the algorithm is known to systematically bias the answer towards a more uniform

TABLE I: Experimental atomic spin populations (μ_B units) obtained using the AOE reconstruction method.

	$H = 4$ T	$H = 7$ T
nitronyl nitroxide		
N1	0.021(6)	0.047(9)
O1	0.026(4)	0.044(5)
N2	0.012(3)	0.057(6)
O2	0.033(4)	0.031(5)
C1	-0.008(4)	-0.033(5)
<i>tert</i> -butyl nitroxide		
N3	0.025(4)	0.040(7)
O3	0.031(4)	0.055(6)
Phenyl C-atoms	$\pm 0.0005(5)$	$\pm 0.015(5)$

distribution.

An alternative reconstruction method known as atomic orbital expansion (AOE)³ lacks the benefit of being model-independent, but is free of such a bias and is better quantified. It involves refining a parameterized model for $S_z(\mathbf{r})$ to best-fit the experimental Fourier data. Its application to F_2PNNNO was founded on previous experiments^{6,7,8,9} and first-principle calculations⁶ for related nitroxides. The NN spin density was described in terms of five atomic populations. It was assumed to be concentrated in p_z Slater-type atomic orbitals of the O, N and apical C atoms, the z axis chosen perpendicular to the corresponding N-O-C planes. Two more parameters were used to quantify the spin density delocalized over the $p_{z'}$ orbitals of the tBuNO N and O atoms, with the z' axis perpendicular to the tBuNO O-N-C plane. One additional parameter was used for the sign-alternating spin density induced in the phenyl ring by virtue of the spin polarization effect.^{8,9} It was assumed to be contained in $p_{z''}$ orbitals of the phenyl's C atoms (z'' is oriented perpendicular to the phenyl plane). The final three parameters were the radial exponents of Slater-type atomic orbitals for the N, O and C atom types. This model yields an excellent least-squares fit to the data collected at $H = 7$ T and $H = 4$ T, with $\chi^2 = 1.09$ and $\chi^2 = 1.20$, respectively. Figure 2 is an isosurface representation of the resulting 3-dimensional spin density distribution in the tetramer at $H = 7$ T. Individual atomic spin populations obtained in the refinement are listed in Table I.

A very good measure of the AOE's reliability is its result for the total tetramer magnetization: $m = 0.48(2)\mu_B$ and $m = 0.28(2)\mu_B$, for $H = 7$ T and $H = 4$ T, respectively, at $T = 10$ K. These values are consistent with existing bulk susceptibility data, and agree well with a thermodynamic quantum-mechanical calculation for a single tetramer: $m = 0.59\mu_B$ and $m = 0.32\mu_B$, respectively. With this assurance of the validity of our approach, we can finally obtain experimental estimates for the imbalance between the NN and tBuNO spin populations: $R = 1.53(3)$ and $R = 1.51(2)$, for $H = 7$ T and $H = 4$ T, based on AOE model refinements.

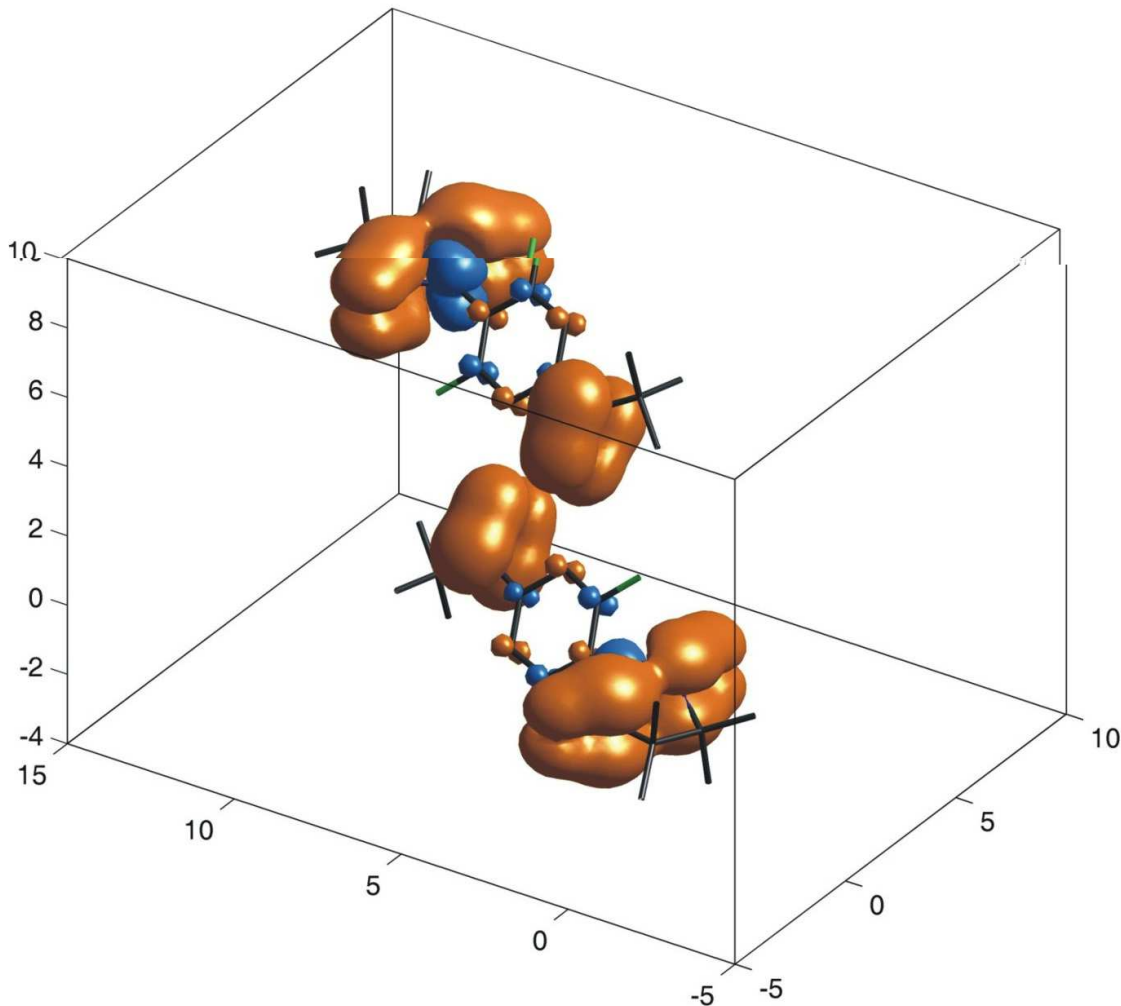


FIG. 4: (Color online) Experimental spin density distribution in a F_2PNNNO spin-tetramer at $H = 7$ T and $T = 10$ K, as reconstructed using orbital model refinement (see text). The isosurfaces are drawn at $1 \times 10^{-3} \mu_B/\text{\AA}^3$ (orange) and $-1 \times 10^{-3} \mu_B/\text{\AA}^3$ (blue) levels. The axes show cartesian coordinates in Angstroms.

IV. DISCUSSION

A value $R > 1$ signifies a reduction of *uniform* induced magnetization around an *antiferromagnetic* bond in the tetramer, and is to be expected. What is important though, is that this effect is hugely magnified by quantum correlations. In a classical magnet with similar exchange constants, all spins would align themselves in the (x, y) plane and tilt slightly in the field (z) direction. It is easy to show that the resulting imbalance in $S_z(\mathbf{r})$ would be an order of magnitude smaller: $R_{\text{classical}} \approx 1 + |J_{\text{AF}}|/4|J_{\text{F}}| = 1.04$.

The quantitative agreement between experiment and direct diagonalization calculations is an important microscopic validation of the model Heisenberg Hamiltonian that was initially hypothesized based on bulk measurements alone.² In fact, our measurements can be viewed as a direct experimental determination of $J_{\text{F}}/J_{\text{AF}}$ in

F_2PNNNO . In addition, these experiments help understand the microscopic interactions within the F_2PNNNO molecule. In Fig. 3, note the negative density in the vicinity of the apical carbon atom of the NN group. This large negative spin population⁸ plays a key role in the ferromagnetic intra-molecular coupling J_{F} . It is a part of a sign-alternating spin density wave that propagates across the phenyl ring and connects the positively populated N sites of the NN and tBuNO fragments over a large distance. This density-wave mechanism is analogous to Ruderman-Kittel-Kasuya-Yosida interactions in metals.^{10,11}

V. CONCLUDING REMARKS

Field-induced spin distributions in quantum magnets are strongly affected by quantum correlations. They can

be directly probed by polarized neutron diffraction and carry valuable information on the system. A very promising avenue for future work are similar experiments on F_2PNNNO conducted at low temperature in the magnetization plateau phase $H > H_{c2}$ and in the inter-plateau region $H_{c1} < H < H_{c2}$. In these regimes the system is expected to be ordered in three dimensions due to inter-tetramer interactions. How does transverse long-range order influence the distribution of S_z , and is in any different from that in effectively isolated tetramers, as studied in this work?

Acknowledgments

The authors thank Dr. E. Ressouche (CEA Grenoble) for his expert assistance with the data analysis

software. Work at ORNL was funded by the United States Department of Energy, Office of Basic Energy Sciences- Materials Science, under Contract No. DE-AC05-00OR22725 with UT-Battelle, LLC. This work was supported in part by Grant-in-Aid for Scientific Research (B) No.18350076 and on priority Areas "High Field Spin Science in 100T" (No.451) from the Ministry of Education, Culture, Sports, Science and Technology (MEXT) of Japan.

* Electronic address: zheludevai@ornl.gov

¹ Y. Hosokoshi, K. Takizawa, H. nakano, T. Goto, M. takahashi, and K. Inoue, *J. Magn. Magn. Mater.* **177-181**, 634 (1998).

² Y. Hosokoshi, Y. Nakazawa, and K. Inoue, *Phys. Rev. B* **60**, 12924 (1999).

³ B. Gillon and J. Schweizer, *Molecules in physics, Chemistry and Biology* (Kluwer, 1989), p. 111.

⁴ R. J. Papoular and B. Gillon, *Europhys. Lett* **13**, 429 (1990).

⁵ R. J. Papoular, A. Zheludev, E. Ressouche, and J. Schweizer, *Acta Cryst.* **A51**, 295 (1995).

⁶ A. Zheludev, V. Barone, M. Bonnet, B. Delley, A. Grand,

E. Ressouche, P. Rey, R. Subra, and J. Schweizer, *J. Am. Chem. Soc.* **116**, 2019 (1994).

⁷ A. Zheludev, M. Bonnet, E. Ressouche, J. Schweizer, M. Wan, and H. Wang, *J. Magn. Magn. Mater.* **135**, 147 (1994).

⁸ M. S. Davis, K. Morokuma, and R. W. Kreilick, *J. Am. Chem. Soc.* **94**, 5588 (1972).

⁹ J. W. Neely, G. F. Hatch, and R. W. Kreilick, *J. Am. Chem. Soc.* **96**, 652 (1974).

¹⁰ M. A. Ruderman and C. Kittel, *Phys. Rev.* **96**, 99 (1954).

¹¹ K. Yosida, *Phys. Rev.* **106**, 893 (1957).